Design analysis of DC electromagnetic pump for liquid sodium–CO2 reaction experimental characterization

Authors: Lee, G., & Kim, H.R*.

Journal Information:

- **Journal:** Annals of Nuclear Energy
- **Year:** 2017
- **Volume:** 109
- **Pages:** 490-497
- **DOI:** https://doi.org/10.1016/j.anucene.2017.05.054

Design analysis of DC electromagnetic pump for liquid sodium–CO_2 reaction experimental characterization

Geun Hyeong Lee, Hee Reyoung Kim*

Ulsan National Institute of Science and Technology, Department of Nuclear Engineering, Ulsan 689-798, Republic of Korea

Abstract

A DC electromagnetic pump with a rectangular channel was optimally designed and fabricated for studying the reaction between liquid sodium and carbon dioxide (CO_2) gas in a sodium fast reactor. Heat exchange using CO_2 gas has recently been proposed for the secondary sodium loop of the sodium fast reactor being developed in Korea because of the strong chemical reaction between liquid sodium and water. A DC conduction-type electromagnetic pump with a rectangular channel was selected to circulate liquid sodium in the experimental test loop for the sodium–CO_2 reaction. Electromagnetic force, which was generated by the Lorentz force of an electrical equivalent circuit, was used to drive the liquid sodium. The developed pressure of the pump was investigated using optimization of the geometrical and electromagnetic variables of the pump considering Lorentz force, electromotive force, and hydraulic loss in the narrow channel of the pump. The characteristics of the developed pressure were studied with respect to the flow rate, and the pump was fabricated using the optimized design specifications. The distributions of current and magnetic flux density in the narrow channel were calculated for the fabricated DC electromagnetic pump with a flow rate of 3 L/min and developed pressure of 0.05 bar, operated at a temperature of 300℃. A comparative analysis of the performance of the designed pump was investigated by considering the fringe effects and Lorentz force using both the equivalent circuit method and numerical analysis.

Keywords: Rectangular DC electromagnetic pump, fringe effects, current distribution, magnetic flux density distribution, developed pressure, sodium–CO_2 reaction test loop.

NOMENCLATURE

B	Magnetic flux density [T]
$\vec{B}$	Magnetic flux density vector [T]

D	Equivalent hydraulic diameter [m]
E_p	Electromotive force [V]
$\vec{E}$	Electric field vector [T]
f_d	Darcy friction factor
H_d	Pump duct height, excluding the wall thickness, along the permanent magnet direction [m]
i_f	Fringe current [A]
i_t	Total input current [A]
i_p	Liquid metal flowing current [A]
i_s	Pump wall current perpendicular to the electrode stub direction [A]
i_{ver}	Current perpendicular to the electrode stub direction [A]
$\vec{J}$	Current density vector [A/m^2]
K_1	Loop friction loss factor
K_2	Fringe factor
L	Length of pump duct [m]
Q	Flow rate [m^3/s]
R_e	Reynolds number
R_f	Fringe resistance [Ω]
R_o	Outer resistance [Ω]
R_p	Liquid sodium resistance [Ω]
R_s	Pump wall resistance perpendicular to the electrode stub direction [Ω]
R_{ver}	Resistance perpendicular to the electrode stub direction [Ω]
t_h	Thickness of the pump wall [m]
T	Temperature [K]
V_t	Input voltage of the pump duct [V]
v	Mean velocity of fluid [m/s]
$\vec{v}$	Velocity vector of fluid [m/s]
W_d	Pump duct width, excluding the wall thickness, along the electrode stub direction [m]
ε_s	Roughness of stainless steel [m]
η	Efficiency

μ	Permeability of material [H/m]
ν	Kinematic viscosity [m^2/s]
ρ_s	Resistivity of liquid sodium [$\Omega \cdot m$]
ρ'	Density of material [kg/m^3]
ρ'_s	Density of liquid sodium [kg/m^3]
σ	Electrical conductivity of material [$1/\Omega \cdot m$]
ΔP	Total developed pressure [Pa]
ΔP_h	Hydraulic pressure loss in the pump [Pa]
ΔP_E	Pressure loss due to electromotive force [Pa]
ΔP_L	Developed pressure due to Lorentz force [Pa]
ΔP_s	System pressure loss [Pa]

1. Introduction

Electromagnetic pumps have been employed for transporting various liquid metals with high electrical conductivity, including liquid sodium in a sodium fast reactor. A DC electromagnetic pump moves liquid metal using the Lorentz force generated from an independent driving current and the magnetic field perpendicular to the driving current. A DC electromagnetic pump with a rectangular channel was selected for the circulation of liquid sodium in the reaction test loop between sodium and carbon dioxide (CO_2) gas (Lee, 2014) because of its structural simplicity and compactness, which make the design suitable for this limited space application.

However, the DC electromagnetic pump requires a relatively high input current compared to induction-type electromagnetic pumps that develop pressure owing to the induced current and magnetic field generated from an externally supplied current source. The input current passing through the pole of the DC electromagnetic pump is one of the parameters that affect the developed pressure. The magnetic field from a pole of finite length and width affects the generation of electromagnetic force. Thus, the developed pressure depends on the geometrical variables of channel height, width, and length, as well as the electromagnetic variables of input current and magnetic field. Moreover, the distributions of the current and magnetic field in the narrow rectangular channel should be analyzed by considering the fringe effects to optimally design the DC electromagnetic pump for implementation in the test loop of the sodium fast reactor.

In the present study, the variables for a DC electromagnetic pump, which needs to operate at a temperature of 300℃ with a flow rate of 3 L/min and developed pressure of 0.05 bar, were optimized to maximize the developed pressure while minimizing the input current. The developed pressure—given as a function of the

geometrical and electromagnetic input variables—was derived using an equivalent circuit. The fringe effects of the current and magnetic field (Baker, 1987), which could influence the developed pressure of the pump, were analyzed, and the design of the pump was optimized. The pump was then fabricated using the optimized design specifications.

2. Analysis of the DC electromagnetic pump with a rectangular channel

The schematic of the DC conduction electromagnetic pump with a rectangular channel is shown in Fig. 1. The electromagnetic pump could be divided into three parts: the electrode, permanent magnet, and pump duct. The developed pressure of the pump was obtained from the Lorentz force, i.e., the product of the externally supplied current and the magnetic field perpendicular to the current. Here, the current flowed through the electrode connected to the power supply, and the magnetic field was driven by an Sm_2Co_{17} permanent magnet. Electrical equivalent circuits were adopted for the analysis of this pump, as shown in Fig. 2 (Nashine, 2007). The equations for the pump were obtained using Kirchhoff's law and Ohm's law. First, from Kirchhoff's law, the current flowing perpendicular to the electrode stub direction i_{ver} was expressed as the sum of the fringe current i_f and the current passing through the duct wall perpendicular to the electrode stub direction i_s:

$$i_{ver} = i_f + i_s \tag{1}$$

The total current i_t was obtained by adding the current flowing in the liquid metal i_p to the current flowing perpendicular to the electrode stub direction i_{ver}:

$$i_t = i_p + i_{ver} \tag{2}$$

By applying Ohm's law and substituting the outer resistance R_o, fringe resistance R_f, and pump wall resistance perpendicular to the electrode stub direction R_s related with the liquid sodium resistance R_p, we obtained a relation for the resistance perpendicular to the electrode stub direction R_{ver}:

$$\frac{1}{R_{ver}} = \frac{1}{R_f} + \frac{1}{R_s} \tag{3}$$

$$R_o i_t + R_{ver} i_{ver} = R_o i_t + R_p i_p + E_p = V_t, \tag{4}$$

where V was the input voltage of the pump duct. Here, E_p was the electromotive force of the pump duct that disturbed the Lorentz force generation:

$$E_p = BW_d v, \tag{5}$$

where B was the magnetic flux density, W_d was the pump duct width along the electrode stub direction, and v was the mean velocity of the fluid. The developed pressure derived by the Lorentz force ΔP_L and its relation with the current i_p and magnetic field B that generate the liquid metal flow was represented by

$$\Delta P_L = \frac{B}{H_d} i_p, \tag{6}$$

where H_d was the pump duct height along the permanent magnet direction. The current passing through the liquid metal in the channel was obtained by combining Eq. (2), Eq. (4), and Eq. (5) and by eliminating R_o and i_{ver}:

$$i_p = \frac{R_{ver} i_t - B W_d v}{R_p + R_{ver}} \tag{7}$$

The hydraulic pressure loss ΔP_h (Crane Co, 1988) of the pump duct was calculated using the Darcy–Weisbach formula (Ohse, 1985) as

$$\Delta P_h = \frac{f_d \rho'_s L v^2 (W_d + H_d)}{4 W_d H_d}, \tag{8}$$

where L was the length of the pump duct and ρ'_s was the density of liquid sodium. The friction coefficient f_d (Haaland, 1983) was expressed as a function of the Reynolds number Re (Grosse, 1966), the roughness of stainless steel ε_s, and the hydraulic diameter D from the Colebrook–White equation for turbulent flow:

$$\frac{1}{\sqrt{f_d}} = -1.8 \log_{10}\left[\frac{6.9}{Re} + \left(\frac{\varepsilon_s}{3.7D}\right)^{1.11}\right] \tag{9}$$

Substituting Eq. (7) in Eq. (6) and considering the hydraulic effects represented in Eq. (8), the developed pressure ΔP and total current i_t of the DC electromagnetic pump were represented, respectively, by

$$\Delta P = \frac{B i_t R_{ver}}{(R_{ver} + R_p) H_d} - \frac{B^2 Q}{(R_{ver} + R_p) H_d^2} - \frac{f_d \rho'_s L Q^2 (W_d + H_d)}{4 (W_d H_d)^3} \quad \text{and} \tag{10}$$

$$i_t = \left(\Delta P + \frac{B^2 Q}{(R_{ver} + R_p) H_d^2} + \frac{f_d \rho_s L Q^2 (W_d + H_d)}{4 (W_d H_d)^3}\right) \frac{(R_{ver} + R_p)}{R_{ver}} \frac{H_d}{B}, \tag{11}$$

where $v = \frac{Q}{W_d H_d}$, Q was the flow rate, ρ_s was the resistivity of liquid sodium, t_h was the thickness of the pump wall, and

$$R_p = \frac{\rho_s W_d}{H_d L} \tag{12}$$

$$R_s = \frac{\rho_s W_d}{2 t_h L} \tag{13}$$

$$R_f = \frac{\rho_s}{K_2 H_d} \tag{14}$$

The fringe current i_f was given as

$$i_f = \frac{K_2 H_d (i_p R_p + E_p)}{\rho_s} \tag{15}$$

where the experimentally determined fringe factor K_2 was equal to 0.4 (Baker, 1987). The pressure loss in the test loop ΔP_s was proportional to the square of the flow velocity and was expressed as a function of flow rate as

$$\Delta P_S = K_1 Q^2, \tag{16}$$

where the proportionality constant K_1 was the loop friction loss factor. The operating point was formed when the developed pressure of the pump was equal to the pressure loss of the test loop of the experimental system. Therefore, the flow rate can be derived from the following quadratic equation obtained by combining Eq. (10) and Eq. (16):

$$\left(K_1 + \frac{f_d \rho'_s L(W_d + H_d)}{4(W_d H_d)^3}\right) Q^2 + \left(\frac{B^2}{(R_{ver} + R_p) H_d^2}\right) Q - \frac{B i_t R_{ver}}{(R_{ver} + R_p) H_d} = 0 \tag{17}$$

The hydraulic efficiency of the pump was defined by the ratio of hydraulic power to electrical input power as

$$\eta = \frac{\Delta P Q}{i_t V_t} \tag{18}$$

where

$$V_t = R_o i_t + R_{ver} i_{ver} \tag{19}$$

The developed pressure was analyzed at different heights and widths of the pump channel and different input currents.

When the width of the electrode and pole piece of the magnetic field are finite, the magnetic field and current in the channel of the pump were obtained by solving the magnetohydrodynamic (MHD) equations given by Ampere's law, Faraday's law, Ohm's law, along with equations for magnetic induction, zero divergence on the magnetic field, and the Navier–Stokes equation as represented in Eq. (20)–(25).

$$\nabla \times \vec{B} = \mu \vec{J} \tag{20}$$

$$\nabla \times \vec{E} = -\frac{\partial \vec{B}}{\partial t} \tag{21}$$

$$\vec{J} = \sigma(\vec{E} + \vec{v} \times \vec{B}) \tag{22}$$

$$\frac{\partial \vec{B}}{\partial t} = \nabla \times \left(\vec{v} \times \vec{B}\right) + \frac{1}{\sigma\mu}\nabla^2\vec{B} \tag{23}$$

$$\nabla \cdot \vec{B} = 0 \tag{24}$$

$$\frac{\partial \vec{v}}{\partial t} + (\vec{v} \cdot \nabla)\vec{v} = -\frac{1}{\rho'}\nabla\vec{P} + \nu\nabla^2\vec{v} + \frac{1}{\rho'}\vec{J} \times \vec{B} \tag{25}$$

Here, $\vec{B}$ is the magnetic flux density vector, $\vec{J}$ is the current density vector, $\vec{E}$ is the electric field vector, μ and σ are the permeability and electrical conductivity of the material, respectively, $\vec{v}$ is the velocity vector of the fluid, and ν is the kinematic viscosity. The normal component of the magnetic flux density at the interface between the permanent magnet and the non-magnetic media of the pump was continuous, and the tangential component of the magnetic field intensity was also continuous. This set of six equations (Eq. (20)–(25)) was solved using the ANSYS code to find the magnetic field and current density. The fringe effects were analyzed from the distributions of the current and magnetic field. As a result, the electromagnetic force generated in the channel of the pump with an electrode and magnet of finite dimensions was obtained by considering the fringe effects.

3. Result and Discussion

The width (W_d) and height (H_d) of the DC electromagnetic pump with a rectangular channel were optimized to maximize the developed pressure for liquid sodium circulation in the sodium–CO_2 reaction test loop, as shown in Fig. 3. An equivalent circuit was used for the optimization, where the length (L) of the pump was set to 0.09 m based on the space in which the pump was to be installed and the input current was 116 A. As the width of the pump was increased, the electromagnetically developed pressure slowly decreased owing to the increase in resistance, while the hydraulic pressure rapidly decreased. In Fig. 4, the total developed pressure of the pump rapidly increased to its maximum and then slowly decreased as the width of the pump was increased at various input currents of 80 A, 120 A, 160 A, and 200 A. To reach the required developed pressure of 0.05 bar, the width of the pump was optimized to 0.0384 m for a fixed length of 0.09 m, as shown in Fig. 4. As shown in Fig. 5, to further maximize the developed pressure when the width and length of the pump were fixed at 0.0384 m and 0.09 m, respectively, the height of the pump was required to be between 0.001 m and 0.002 m;

specifically, the optimized height of the pump was 0.0018 m. The length of the pump was determined as 0.09 m considering the current density permissible in copper electrodes, even though the developed pressure reached its maximum at a point between 0.04 m and 0.07 m of the pump length when the current was higher than 80 A, as shown in Fig. 6. Consequently, the channel of the pump had a length of 0.09 m, width of 0.0384 m, and a height of 0.0018 m, and the thickness of the channel was 0.001 m (Gahan, 1970). At these dimensions, the input current of 116 A resulted in a developed pressure of 0.05 bar.

The Sm_2Co_{17} permanent magnets of thickness 0.006 m were selected to satisfy temperature condition to generate an external magnetic field of 0.172 T at the required input current of 116 A, where the hydraulic efficiency was approximately 27.2%. The flow rate increased as the input current increased, as shown in Fig. 7. The total developed pressure, the pressure losses from the electromotive force and hydraulic pressure, and the developed pressure from Lorentz force were plotted against the change in input current, as shown in Fig. 8. A developed pressure of 0.082 bar was generated from the Lorentz force, while pressure losses were induced by the counter electromotive force (0.028 bar loss) and hydraulic pressure (0.004 bar), resulting in a total developed pressure of 0.05 bar at the nominal input current of 116 A. The characteristics of the developed pressure are shown with respect to the flow rate in Fig. 9.

The pump was fabricated according to the optimized design specifications listed in Table 1, as shown in Fig. 10. A DC power supply with a maximum current of 200 A and voltage of 5 V was employed. Using Eq. (2), Eq. (7), and Eq. (15) in the equivalent circuit of the pump, the current flowing in the liquid sodium in the completed pump channel was found to be 48.7% of the total input current, while the fringe and wall currents were 24.9% and 26.4%, respectively. The fringe effects on the current and magnetic field were important factors affecting the developed pressure of the pump.

Using ANSYS code, the distribution of the current density was obtained, as shown in Fig. 11 and Fig. 12. In Fig. 11, the contour of the current density distribution on the plane of height and length showed that the current was constant along the height, whereas current reached its maximum in the central region of the electrode of length 0.09 m. In Fig. 12, the current density at the center of the width and height of the channel decreased toward the outside of the electrode and was almost zero at a distance of 0.1 m from the center of the electrode; the current density was constant over 60% of the area of the pump duct, strictly showing a maximum at the center of the pump duct. Finally, there were two types of fringe current effects: an “out of duct” current parallel

to the direction of the input current along the electrode stub, and a current perpendicular to the direction of the input current along the electrode stub. The “out of duct” current was 17.84% of the total current passing through the pump duct, while the current flowing perpendicular to that in the electrode stub was 0.0354%, i.e., negligible. Finally, 17.88% of the current flowing in the duct was thought to be leaked without contributing to the generation of electromagnetic force required for the flow of liquid sodium. Consequently, the ratios of the current flowing along the liquid sodium inside the channel to the input current, fringe current, and duct wall current were 60.40%, 13.16%, and 26.44%, respectively. Thus, from the ANSYS code analysis when the inhomogeneity of the current distribution of the electrode was considered, the fringe current reached approximately 13.16% of the total current, in contrast to the fringe current of 24.94% from the equivalent circuit analysis on the constant current. In considering the fringe effect of the magnetic field, some of the fringe current was thought to contribute to the generation of electromagnetic force, where the magnetic field would not be completely zero on the outside of the pole piece.

In Fig. 13 and Fig. 14, the distribution of the magnetic field perpendicular to the current is shown along the direction of flow when the input current was 116 A. The magnetic field distribution at the center of the width and height of the channel was obtained using ANSYS code when the Sm_2Co_{17} permanent magnets were arranged on both sides of the channel, as shown in Fig. 13. The magnetic flux density was positive on the inside of the pole piece of the magnet, showing peaks at both edges, and the mean value of the magnetic flux density in the pole piece was 0.172 T. The direction of magnetic field was downward in the, majority of the flow channel, except for the ends, where the direction of the magnetic field was upward, as represented in Fig. 14, because flux line was generated around the permanent magnet causing opposite direction magnetic field as represented in Fig. 15(b). Therefore, the magnitude of magnetic flux density was negative outside the pole piece at both ends, causing a force in the direction opposite to the flow of the liquid sodium.

The magnetic flux density was measured using a Gauss meter along the direction of sodium flow at the flow channel of the manufactured DC electromagnetic pump, as represented in Fig. 10. The distribution of the magnetic flux density obtained from calculations and measurements are represented in Fig. 15(a). The actual magnetic field along the length of the pole piece positively deviated from the calculated magnetic field, which indicated a distortion error in the electromagnetic force. The generated electromagnetic force density was plotted from the vector product of current density and magnetic flux density, as shown in Fig. 16. The electromagnetic force was reversely generated at the outside of the pump duct (the pole piece of the permanent

magnet) due to the reversed (upward) direction of magnetic field at that point. The total electromagnetic force was 0.295 N on average, where 0.318 N of the electromagnetic force was on the inside of the pump duct (the pole piece) and -0.023 N of the electromagnetic force was on the outside of pump duct, causing a developed pressure of 0.043 bar. This developed pressure was lower than the developed pressure of 0.082 bar from the equivalent circuit. In this calculation, the fringe effect of the magnetic field as well as that of the current caused a reduction in the force, whereas a constant magnetic field was assumed in the equivalent circuit. The current density reached its maximum at the center of the pump and decreased outward from the center, while the magnetic flux density reached its maximum at the edges of the pump duct with a negative value outside the duct. Therefore, the Lorentz force, $\int \vec{J} \times \vec{B}\, dv$, showed a reduced value of the developed pressure compared with that from the equivalent circuit analysis. In particular, the electromagnetic force (Lorentz force) from the ANSYS code analysis was reduced by 52.4% compared with that from the equivalent circuit analysis, which assumed a constant distribution of current and magnetic field. The reduction in electromagnetic force in the ANSYS code analysis occurred because the magnetic field distribution was not homogeneous in the permanent magnet, as shown in Fig. 15, while the fringe current effect was higher in the equivalent circuit analysis.

4. Conclusion

Optimization of the geometrical variables (width of 0.0384 m, height of 0.001 8 m, and length of 0.09 m) and an electrical variable (input current of 116 A) was performed to obtain a design for a DC electromagnetic pump that required a developed pressure of 0.05 bar and a flow rate of 3 L/min at a temperature of 300℃. The total electromagnetic force was reduced owing to inhomogeneity in the current and magnetic field at the electrode and magnet, even though fringe effects on the current and magnetic field contributed to the generation of electromagnetic force.

References

Baker, R.S., Tessier, M.J., 1987. Handbook of Electromagnetic Pump Technology. Elsevier, New York.

Crane Co., 1988. TP-410 Flow of Fluids through Valves, Fittings, and Pipe. Crane Co, Chicago.

Gahan, J. W., Pileggi, P. T., Powell, A. H., 1970. Primary loop-Electromagnetic pump design. General Electric Co, Ohio.

Gross, A.V., 1966. Kinematic viscosity of metallic mercury, sodium and potassium, over their entire liquid range (i.e., from the melting point to the critical point) and a comparison with Van der Walls' substances. J. Inorg. Nucl. Chem. 28, 31-39, DOI:10.1016/0022-1902(66)80225-7.

Haaland, S.E., 1983. Simple and explicit formulas for the friction factor in turbulent pipe flow. J. Fluids Eng, 105, 89-90, DOI:10.1115/1.3240948.

Lee, Y., Lee. J.I, 2014. Structural assessment of intermediate printed circuit heat exchanger for sodium-cooled fast reactor with supercritical CO_2 cycle. Ann. Nucl. Energy 73, 84-95, DOI:10.1016/j.anucene.2014.06.022.

Nashine, B.K., Dash, S.K., Gurumurthy, K., Kale, U. Sharma, V.D, Prabhaker, R. Rajan, M. Vaidyanathan, G., 2007. Performance testing of indigenously developed DC conduction pump for sodium cooled fast reactor. Indian J. Eng. Mat. Sci. 14, 209-214.hse.

Ohse, R.W., 1985. Handbook of Thermodynamic and Transport Properties of Alkali Metals. Blackwell Scientific Publications, Oxford.

Figure captions

Fig. 1 Diagram of the proposed DC electromagnetic pump with a rectangular channel

Fig. 2 Electrical equivalent circuit of the DC electromagnetic pump with a rectangular channel: (a) basic form, and (b) simplified form.

Fig. 3 Total developed pressure of the DC electromagnetic pump with a rectangular channel versus W_d and H_d at I = 155.06 A and L = 0.09 m.

Fig. 4 Total developed pressure of the DC electromagnetic pump with a rectangular channel versus W_d at H_d = 0.0018 m and L = 0.09 m.

Fig. 5 Total developed pressure of the DC electromagnetic pump with a rectangular channel versus H_d at W_d = 0.0384 m and L = 0.09 m.

Fig. 6 Total developed pressure of the DC electromagnetic pump with a rectangular channel versus L at H_d = 0.0018 m and W_d = 0.0384 m.

Fig. 7 Flow rate on the change of the input current in the DC electromagnetic pump with a rectangular channel.

Fig. 8 Developed pressures and pressure losses on the change of input current in the DC electromagnetic pump with a rectangular channel

Fig. 9 P–Q curve of the DC electromagnetic pump with a rectangular channel considering the fringe effects at I = 155.06 A

Fig. 10 Manufactured DC electromagnetic pump with a rectangular channel and its power supply

Fig. 11 Plain current density distribution of the DC electromagnetic pump with a rectangular channel at a midpoint of W_d

Fig. 12 Linear current density distribution of the DC electromagnetic pump with a rectangular channel at midpoints of W_d and H_d

Fig. 13 Plain magnetic field distribution of the DC electromagnetic pump with a rectangular channel at a midpoint of H_d

Fig. 14 Linear magnetic field distribution of the DC electromagnetic pump with a rectangular channel at midpoints of W_d and H_d

Fig. 15 (a) Magnetic field distributions of the DC electromagnetic pump with a rectangular channel obtained with both simulation and experimental data; (b) Magnetic flux lines of the DC electromagnetic pump

Fig. 16 Generated force density of the DC electromagnetic pump with a rectangular channel at midpoints of W_d and H_d

Table captions

Table 1 Design specifications for the DC electromagnetic pump with a rectangular channel from the analytical solution.

Table 1

	Design variables	Unit	Values
Hydrodynamic	Flow rate (Q)	[m^3/s]	0.00005
	Developed pressure (ΔP)	[bar]	0.05
	Temperature (T)	[K]	573.15
	Velocity (v)	[m/sec]	0.72
	Reynolds number (R_e)		6445
	Fringe Factor (K_2)		0.4
	Pressure loss (ΔP_L)	[bar]	0.004
Geometrical	Height (H_d)	[m]	0.0018
	Width (W_d)	[m]	0.0384
	Length (L)	[m]	0.09
	Thickness (t_h)	[m]	0.001
Electrical	Input current (i_t)	[A]	116
	Input voltage (V_t)	[V]	0.0079
	Efficiency (η)	[%]	27.2

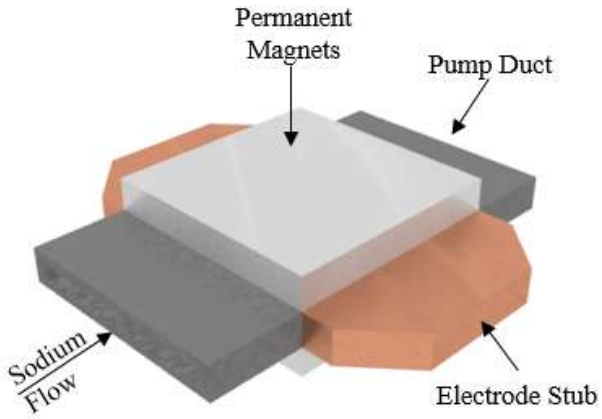

Fig. 1

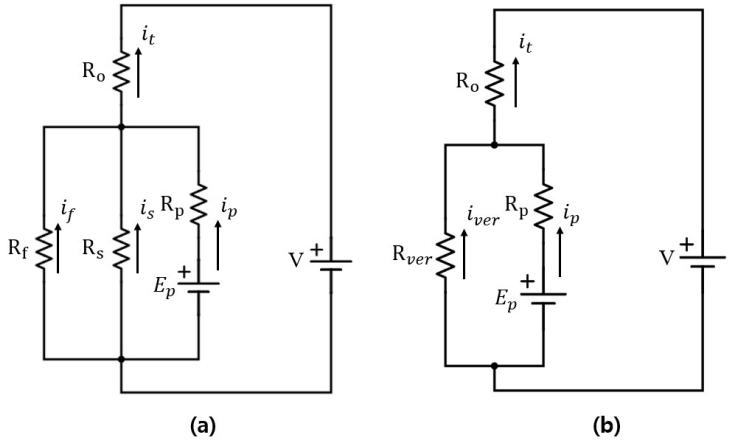

Fig. 2

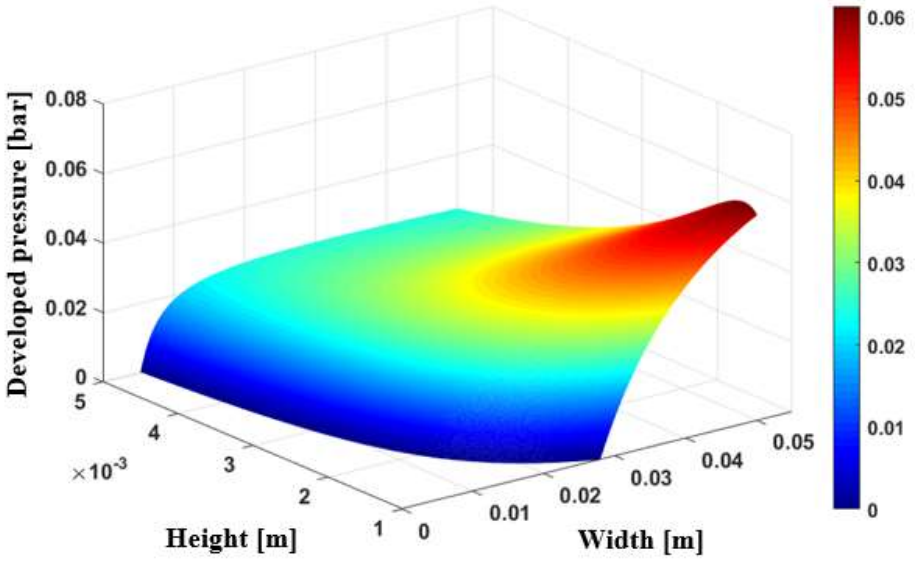

Fig. 3

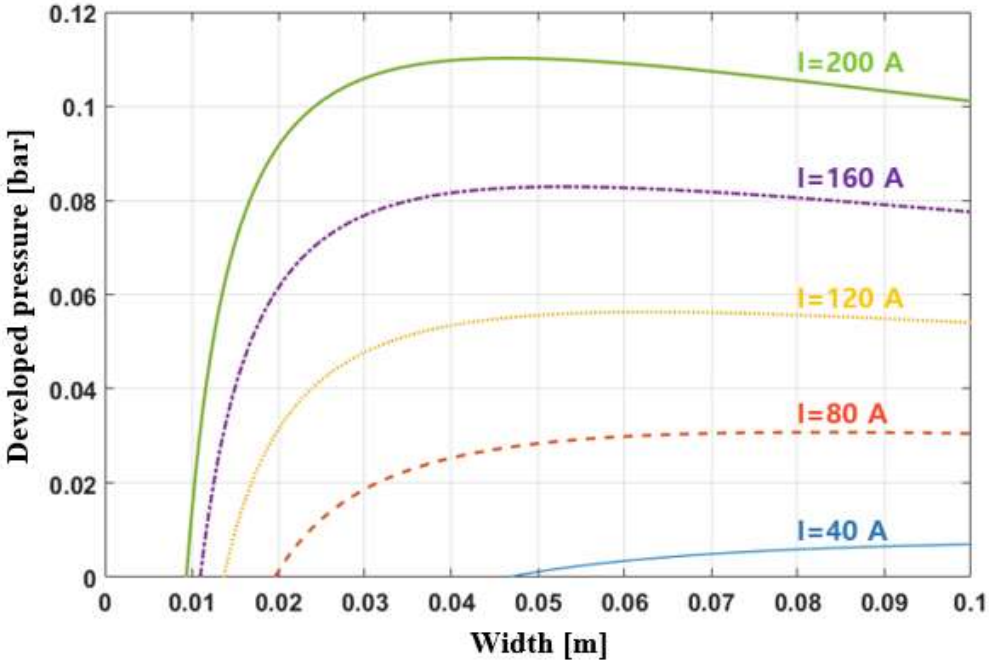
Developed pressure [bar]
Width [m]
I=200 A
I=160 A
I=120 A
I=80 A
I=40 A
0.12
0.1
0.08
0.06
0.04
0.02
0
0.01
0.02
0.03
0.04
0.05
0.06
0.07
0.08
0.09
0.1

Fig. 4

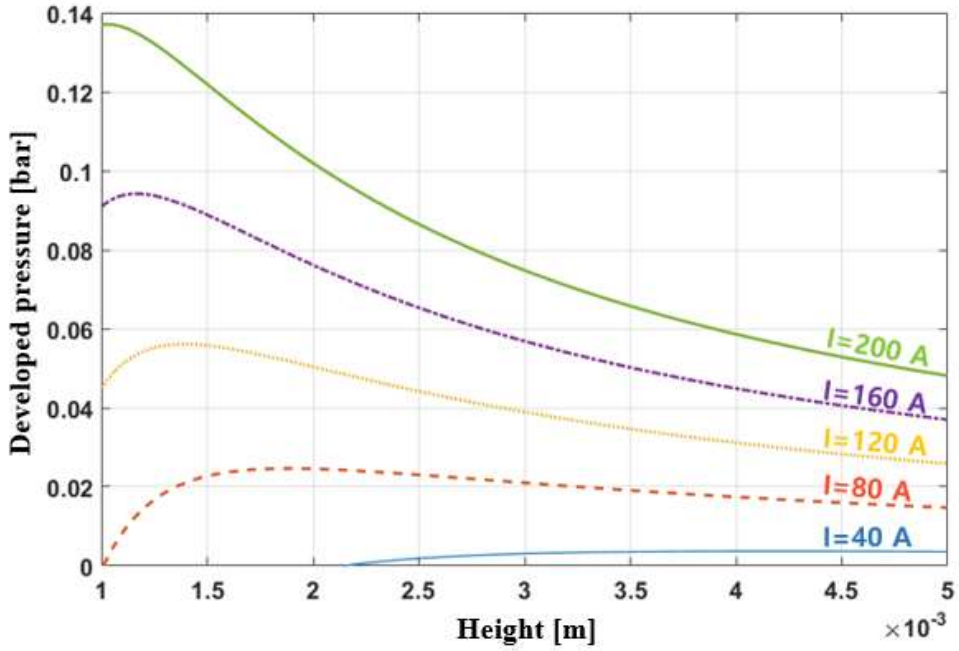
Developed pressure [bar]
Height [m]
×10-3
I=200 A
I=160 A
I=120 A
I=80 A
I=40 A
0.14
0.12
0.1
0.08
0.06
0.04
0.02
0
1
1.5
2
2.5
3
3.5
4
4.5
5

Fig. 5

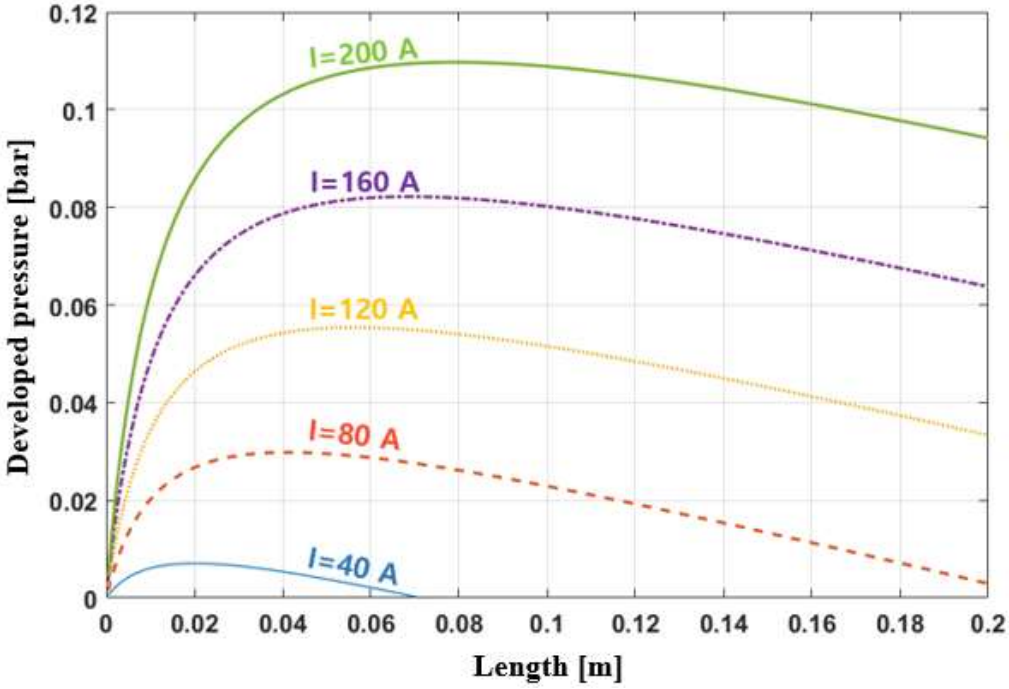
I=200 A
I=160 A
I=120 A
I=80 A
I=40 A
Developed pressure [bar]
Length [m]
0.12
0.1
0.08
0.06
0.04
0.02
0
0.02
0.04
0.06
0.08
0.1
0.12
0.14
0.16
0.18
0.2

Fig. 6

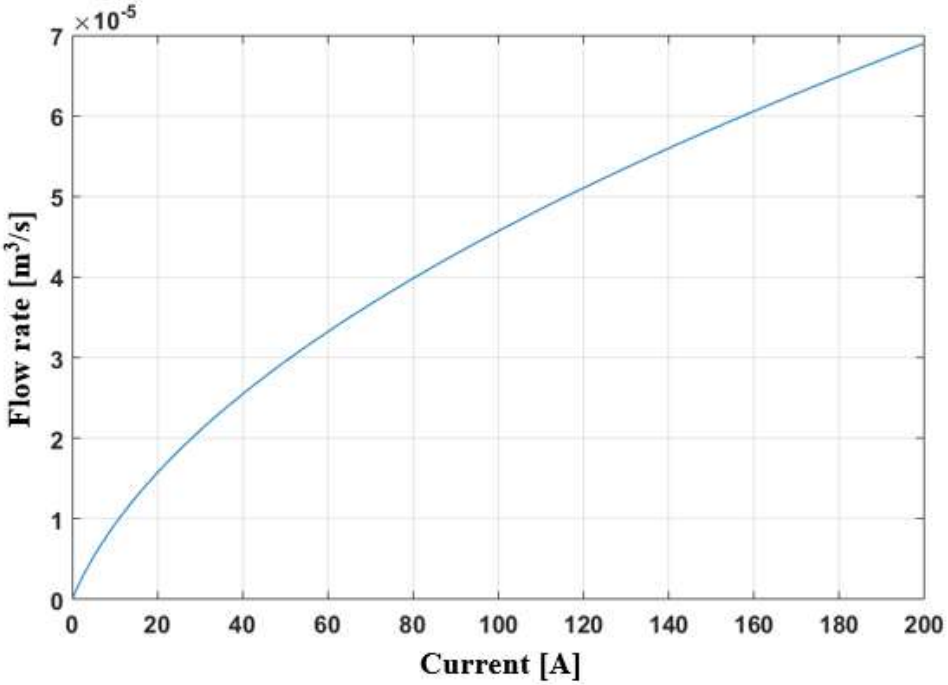
×10-5
Flow rate [m3/s]
Current [A]
7
6
5
4
3
2
1
0
0
20
40
60
80
100
120
140
160
180
200

Fig. 7

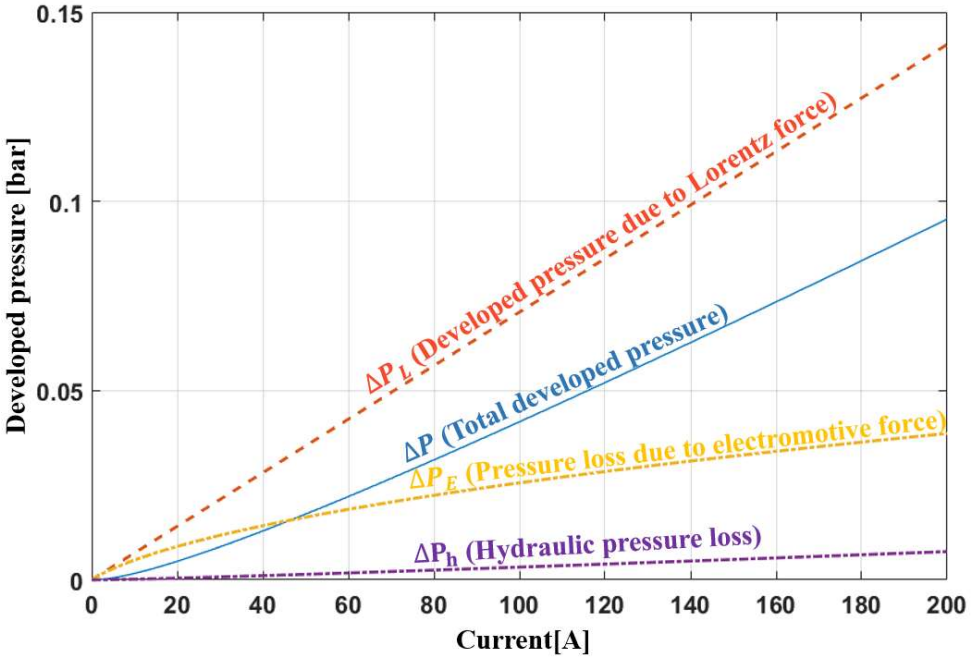
0.15
0.1
0.05
0
Developed pressure [bar]
0
20
40
60
80
100
120
140
160
180
200
Current[A]
ΔP_L (Developed pressure due to Lorentz force)
ΔP (Total developed pressure)
ΔP_E (Pressure loss due to electromotive force)
ΔP_h (Hydraulic pressure loss)

Fig. 8

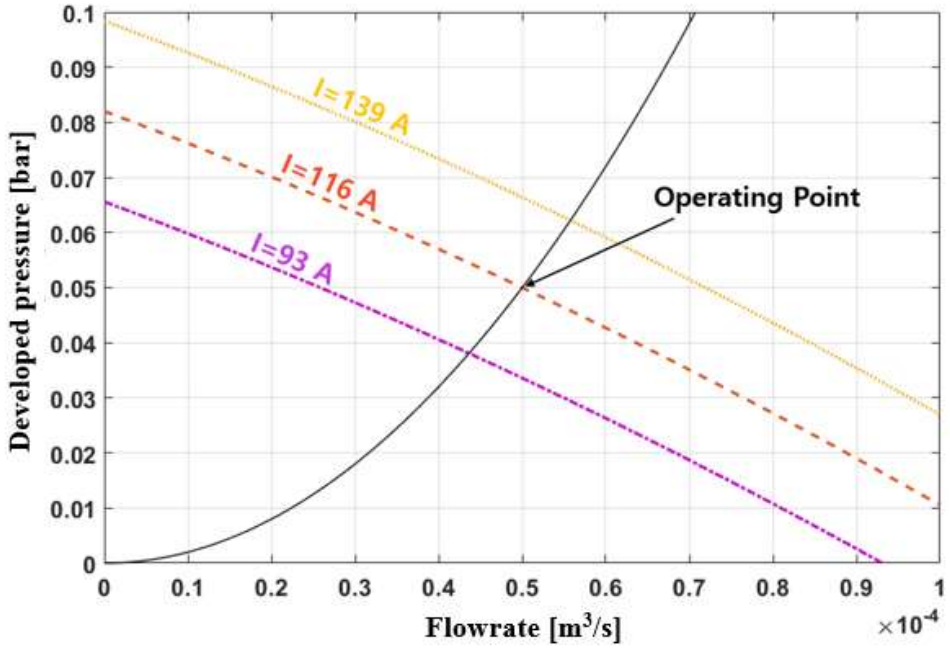
0.1
0.09
0.08
0.07
0.06
0.05
0.04
0.03
0.02
0.01
0
Developed pressure [bar]
0
0.1
0.2
0.3
0.4
0.5
0.6
0.7
0.8
0.9
1
Flowrate [m³/s]
×10⁻⁴
I=139 A
I=116 A
I=93 A
Operating Point

Fig. 9

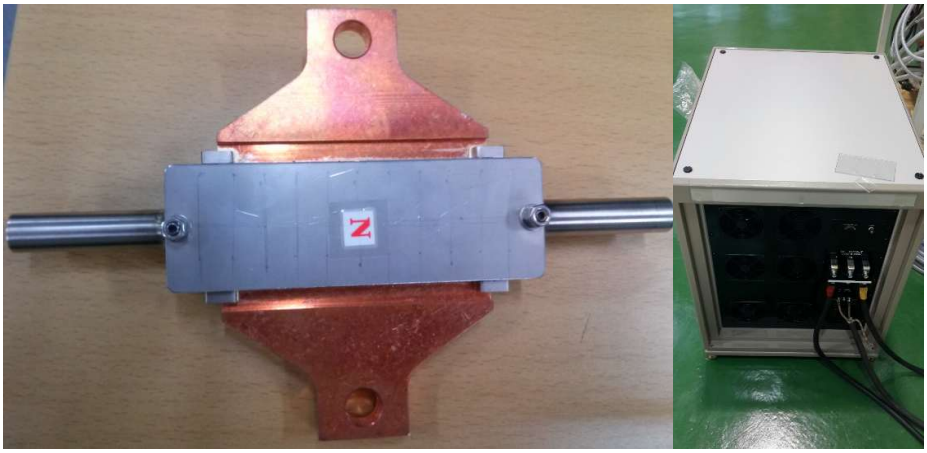

Fig. 10

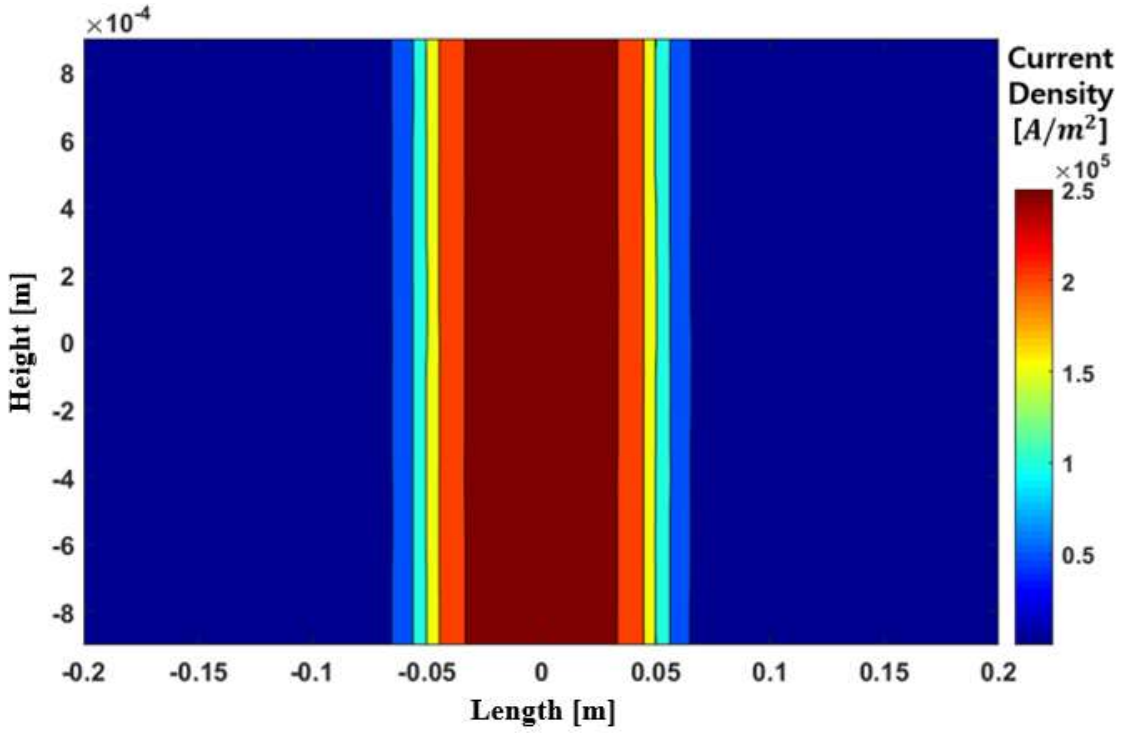
×10^-4
8
6
4
2
0
-2
-4
-6
-8
Height [m]
-0.2
-0.15
-0.1
-0.05
0
0.05
0.1
0.15
0.2
Length [m]
Current Density [A/m^2]
×10^5
2.5
2
1.5
1
0.5

Fig. 11

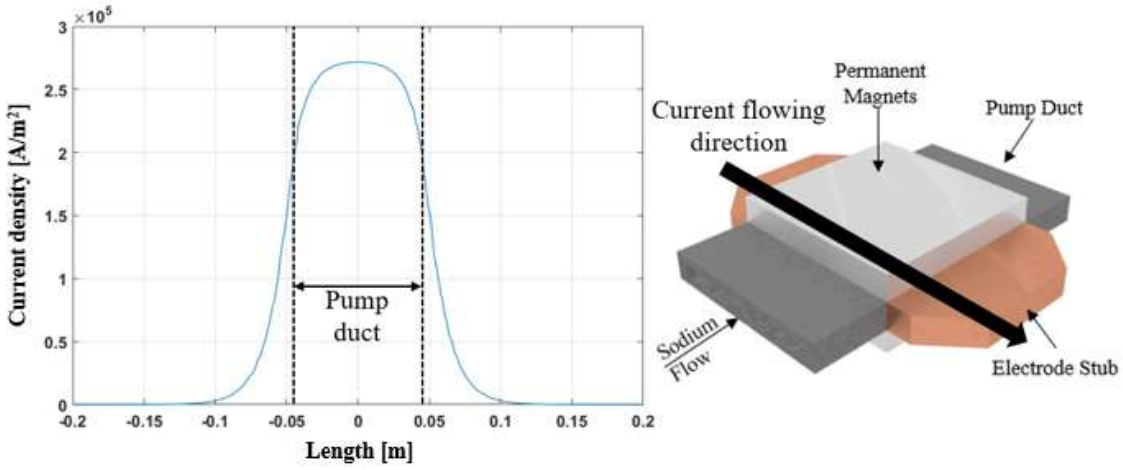
×10^5
Current density [A/m^2]
Length [m]
Pump duct
Current flowing direction
Permanent Magnets
Pump Duct
Sodium Flow
Electrode Stub

Fig. 12

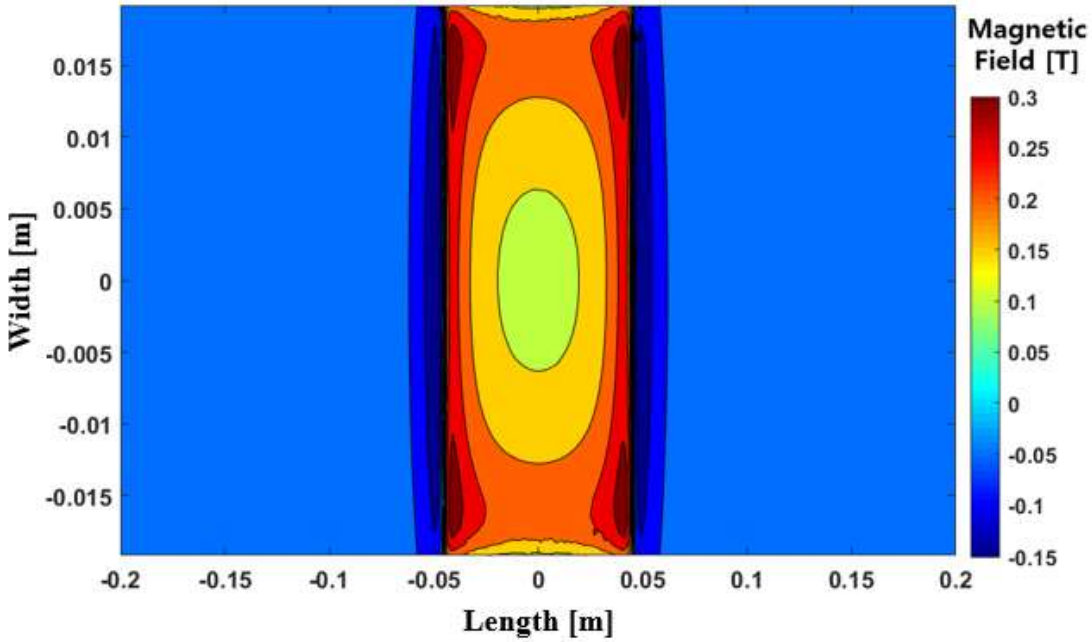
Magnetic Field [T]
Width [m]
Length [m]

Fig. 13

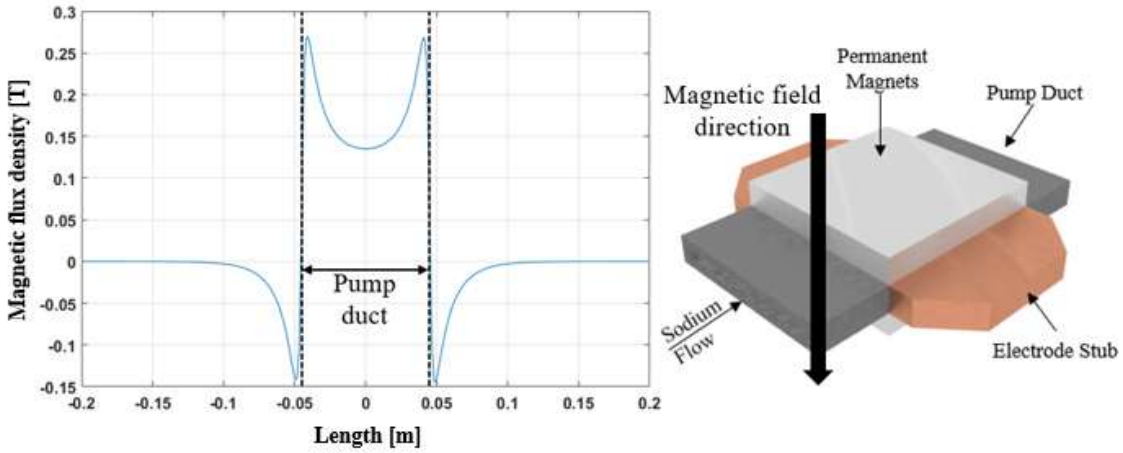
Magnetic flux density [T]
Length [m]
Pump duct
Magnetic field direction
Permanent Magnets
Pump Duct
Sodium Flow
Electrode Stub

Fig. 14

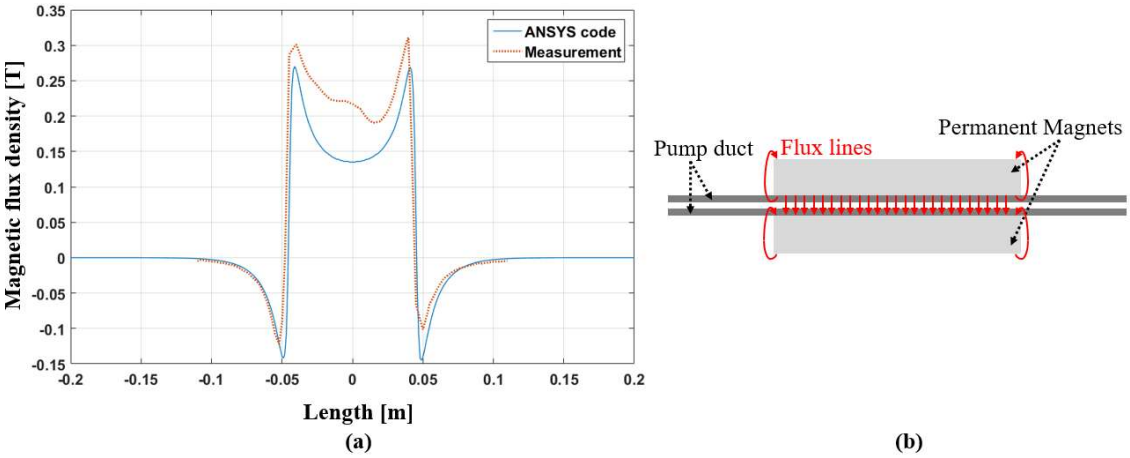
ANSYS code
Measurement
Magnetic flux density [T]
Length [m]
(a)
Pump duct
Flux lines
Permanent Magnets
(b)

Fig. 15

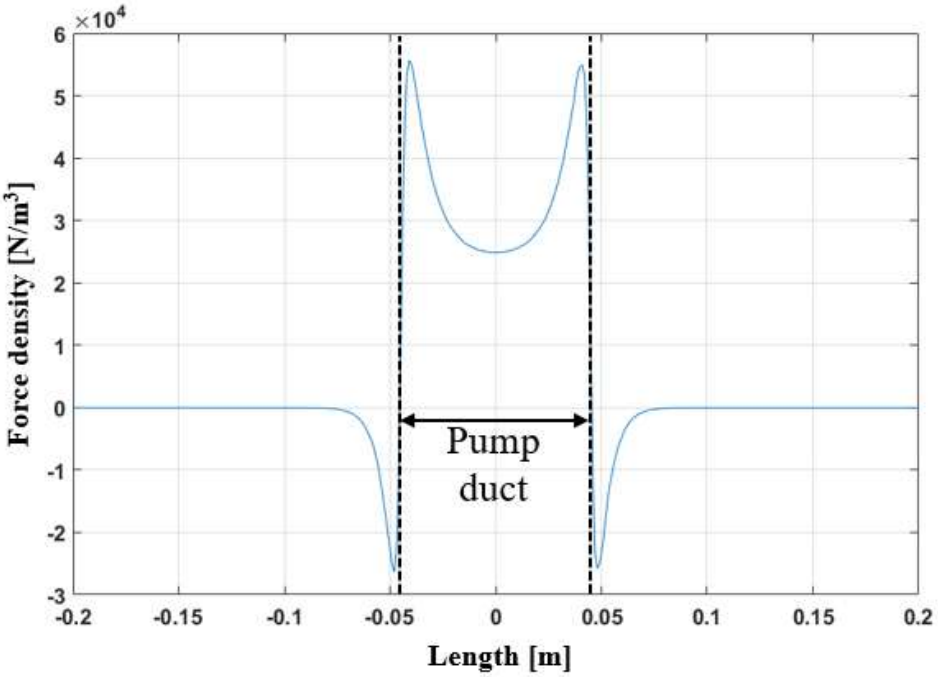
×10^4
6
5
4
3
2
1
0
-1
-2
-3
Force density [N/m^3]
Pump
duct
-0.2
-0.15
-0.1
-0.05
0
0.05
0.1
0.15
0.2
Length [m]

Fig. 16